# Analog information processing at the quantum limit with a Josephson ring modulator

N. Bergeal[1], R. Vijay[1,2], V. E. Manucharyan[1], I. Siddiqi[2], R. J. Schoelkopf[1], S. M. Girvin[1], M. H. Devoret[1]

[1] *Department of Physics and Applied Physics, Yale University, New Haven, Connecticut, 06520-8284 USA. and*

[2] *Department of Physics, University of California, Berkeley CA 94720-7300, USA.*

(Dated: October 22, 2009)

arXiv:0805.3452v2 [cond-mat.mes-hall] 22 Oct 2009

Amplifiers are crucial in every experiment carrying out a very sensitive measurement. However, they always degrade the information by adding noise. Quantum mechanics puts a limit on how small this degradation can be. Theoretically, the minimum noise energy added by a phase preserving amplifier to the signal it processes amounts at least to half a photon at the signal frequency ($\frac{1}{2}\hbar\omega_S$). In this article, we show that we can build a practical microwave device that fulfills the minimal requirements to reach the quantum limit. This is of importance for the readout of solid state qubits, and more generally, for the measurement of very weak signals in various areas of science. We also discuss how this device can be the basic building block for a variety of practical applications such as amplification, noiseless frequency conversion, dynamic cooling and production of entangled signal pairs.

The concept of quantum limited amplification was introduced in the 1950's with the development of the first maser amplifiers[1]. Later, following the work of Haus and Mullen[2], Caves[3] reviewed the subject and introduced a general formalism which includes all linear amplifiers (i. e. an amplifier whose output signal is linearly related to its input signal). His analysis led to a fundamental theorem : a phase preserving amplifier has to add a minimum amount of noise to the signal it processes. The limit is commonly expressed in terms of the minimal temperature of the noise added by an amplifier to the signal

$$T_N^{\text{added}} = \frac{1}{2}\frac{\hbar\omega_S}{k_B} \tag{1}$$

where $\omega_S$ is the angular frequency of the signal. This corresponds to $\frac{1}{2}$ photon added to each signal mode at the input of the amplifier. On the other hand, a phase sensitive amplifier, in which one quadrature is amplified while the other is de-amplified, is submitted to only a lower limit on the product of the noise added to the two quadratures and can squeeze the quantum noise on one quadrature at the expense of extra noise on the other one. Although such amplifiers can look rather appealing because of their ability to operate potentially below the quantum limit (1), they are awkward to use in a wide number of applications where both the phase and amplitude of the signal carry the information. On the other hand, the so-called non-degenerate parametric amplifier, i. e. an amplifier in which a non-linear system[4, 5] with two resonant frequencies is pumped with an oscillatory source has repeatedly been suggested to be a good candidate as a phase preserving amplifier reaching the quantum limit[6, 7]. It operates with two spatially distinct modes, conventionally called the "signal" at frequency $\omega_S$ and the "idler" (a.k.a. the "image") at frequency $\omega_I$. These two modes are coupled in the non-linear system via the "pump" at frequency $\Omega$. The device operates as an amplifier with photon number gain when $\Omega = \omega_S + \omega_I$ or as a frequency converter without photon number gain when $\Omega = |\omega_S - \omega_I|$ [4, 5].

In this article, we will focus on the phase preserving case and show that a practical, non-degenerate parametric amplifier operating in the microwave domain can be realized with a simple circuit involving Josephson tunnel junctions. Because it is minimal in the number of active modes, it should reach the quantum limit. Unlike microwave SQUIDs, which are powered by a DC current bias and operate with incoherent Josephson radiation[8, 9], Josephson parametric amplifiers involve a coherent microwave source. Josephson tunnel junction parametric amplifiers have so far mainly focused on degenerate amplifiers ($\omega_S = \omega_I$) which operate as phase sensitive amplifiers[10, 11, 12] and very little work has been devoted to phase preserving amplifiers. The difficulty of building a practical device matching the theoretical proposals as well as the lack

of applications requiring quantum limited performances contributed to put this field on hold. However, recent progress in quantum information processing using microwave interrogation of solid states qubits[13, 14, 15, 16] gave rise to a growing need for low-noise amplifiers which are sensitive enough to measure the extremely weak signals involved in these new devices and renewed the interest in parametric amplifiers [17, 18, 19, 20]. Also, amplifiers operating near the quantum limit are essential in quantum feedback for sustaining the coherent oscillation of a qubit [21, 22].

**The Josephson ring modulator**

Even at zero temperature, internal dissipation in a device inevitably adds noise to the output signals. Thus, it is important to build a completely dissipationless circuit employing only dispersive elements. The amplifier that we describe here is based on a particularly interesting novel non-linear device, which we call the Josephson ring modulator, by analogy with the ring modulator employing Schottky diodes[23]. The device consists of four nominally identical Josephson junctions forming a ring threaded by a magnetic flux $\Phi$. This magnetic flux induces a fixed, circulating current around the ring. When operated with a bias current lower than their critical current $I_0$, Josephson junctions behave as pure non-linear inductors with inductance $L_J = \varphi_0/(I_0 \cos\delta)$ where $\delta$ is the gauge invariant phase of the junction and $\varphi_0 = \frac{\hbar}{2e}$ is the reduced flux quantum. They are the only known non-linear and non-dissipative circuit elements working at microwave frequencies. The ring has three orthogonal electrical modes coupled to the junctions : two differential ones, $X$ and $Y$, and a common one, $Z$ (Fig 1a). They provide the minimum number of modes for 3-wave mixing.

We introduce the node flux $\Phi_{i=1,..,4}$ defined by

$$V_{i=1,..,4} = \frac{d\Phi_{i=1,..,4}}{dt} \tag{2}$$

where $V_{i=1,..,4}$ are the potentials at ring nodes 1, 2, 3 and 4. The amplitudes of the three modes $X$, $Y$, $Z$ can be chosen as the following combination of nodes fluxes

$$\Phi_X = \Phi_1 - \Phi_2 \quad ; \quad \Phi_Y = \Phi_4 - \Phi_3 \quad ; \quad \Phi_Z = \Phi_1 + \Phi_2 - \Phi_3 - \Phi_4$$

In the case of large area junctions, the charging energy due the intrinsic capacitance of the junctions can be neglected. Hence, the Hamiltonian of the ring is only given by the sum of the Josephson Hamiltonian of each junction $H_J = -E_J \cos\delta_{i=a,b,c,d}$, where $E_J = I_0\varphi_0$ [24]. By rewriting the sum of the Josephson energies as a function of the variables $\Phi_X$, $\Phi_Y$ and $\Phi_Z$

$$H_{\text{ring}} = -4E_J[\cos\frac{\Phi_X}{2\varphi_0}\cos\frac{\Phi_Y}{2\varphi_0}\cos\frac{\Phi_Z}{2\varphi_0}\cos\frac{\Phi}{4\varphi_0} + \sin\frac{\Phi_X}{2\varphi_0}\sin\frac{\Phi_Y}{2\varphi_0}\sin\frac{\Phi_Z}{2\varphi_0}\sin\frac{\Phi}{4\varphi_0}] \tag{3}$$

In figure 1b we plot the energy of local equilibrium states of the Josephson ring modulator as a function of the magnetic flux $\Phi$ when no external currents are applied to the ring. There are 4 stable states satisfying the quantization of the flux through the loop. Although each state is $4\Phi_0$ periodic as a function of the flux, the envelope of the lowest energy state remains $\Phi_0$ periodic as required by gauge invariance ($\Phi_0 = 2\pi\varphi_0$).

Let us now consider the degenerate ground state at $\Phi = \Phi_0/2$ labeled $a$ in figure 1b. For mode intensities $\Phi_X$, $\Phi_Y$ and $\Phi_Z$ much smaller than $\Phi_0$, we can neglect terms of order higher than three and (3) reduces to

$$H_{\text{ring}} = \lambda\Phi_X\Phi_Y\Phi_Z + \mu[\Phi_X^2 + \Phi_Y^2 + \Phi_Z^2] \tag{4}$$

with $\lambda = -2\sqrt{2}\pi^3 E_J/\Phi_0^3$ and $\mu = \sqrt{2}\pi^2 E_J/\Phi_0^2$. Apart from the sought-after pure non-linear coupling term $\Phi_X\Phi_Y\Phi_Z$, the Hamiltonian contains a contamination term which is only quadratic in the fluxes and which therefore only renormalizes the mode frequencies. This powerful result shows that the Josephson ring modulator can perform the operation of mixing 3 orthogonal field modes while producing a minimal number of spurious non-linear effects. The Wheatstone bridge

type of symmetry eliminates most of the unwanted terms in the Hamiltonian, in particular those of the form $\Phi_X^2\Phi_Z$, $\Phi_Y^2\Phi_Z$, $\Phi_X^2\Phi_Y$, $\Phi_Y^2\Phi_X$ which would induce other, unwanted types of mixing ( see below). Note that although $\Phi = \Phi_0/2$ is optimal for maximizing $\lambda$ while keeping the working point stable, it is not a stringent condition. In the following, the differential modes $X$ and $Y$ are used to carry the signal and the idler with symmetric roles while the $Z$ mode is used as the pump.

**The Josephson Parametric Converter**

We now feed the $X$ and $Y$ modes of the Josephson ring modulator through two superconducting resonators. A lumped element representation of the circuit that we have named the Josephson Parametric Converter (JPC) is shown in figures 2a&b. The device contains only purely dispersive elements: superconducting resonators and Josephson junctions. Since it has no internal dissipation, all the noises appearing at the output ports originate from the coupling of the JPC to the external circuits connected at its different ports. There are in fact two possible variations of the circuit depending on whether the ring modulator junctions are in parallel with the voltage of the resonators (Fig. 2a) or in series with the current of the resonators (Fig. 2b). For simplicity and conciseness we treat here only the first case. The second case can be treated by a simple extension of the formalism we present. The Hamiltonian of the two resonators is given by [24, 25] ,

$$H_{\rm res} = \frac{\Phi_X^2}{2L_a} + \frac{Q_X^2}{2C_a} + \frac{\Phi_Y^2}{2L_a} + \frac{Q_Y^2}{2C_a} + H_{\rm damp} \tag{5}$$

where the $\Phi's$ and the $Q's$ are the conjugated fluxes and charges in the inductive and capacitive parts of the circuit, respectively, and where the $L's$ and $C's$ are the associated inductances and capacitances. The damping term $H_{\rm damp}$ arising from the coupling to the external source resistors $R_a$ and $R_b$ could be expressed using the Caldeira-Leggett model [26], which treats dissipation in a quantum circuit, but this detailed description is not of interest here. In addition, each resonator is

submitted to a weak, time-dependent external drive which models the incoming signal (idler). This contribution can be taken into account by introducing the Hamiltonian of the drives [24]

$$H_{\text{drive}} = -\Phi_X \frac{U_1}{R_a}\cos(\omega_1 t + \phi_1) - \Phi_Y \frac{U_2}{R_b}\cos(\omega_2 t + \phi_2) \tag{6}$$

The pump mode is assumed to be so stiffly driven that $\Phi_Z$ can be regarded as an imposed oscillating classical field, which does not suffer backaction from its coupling to the other modes.

Therefore, the total Hamiltonian of the JPC is given by

$$H_{JPC} = H_{\text{res}} + H_{\text{ring}} + H_{\text{drive}} \tag{7}$$

In the following, we consider the case where the pump is driven with two tones at frequencies $\Omega_\sigma = \omega_1 + \omega_2$ and $\Omega_\delta = \omega_1 - \omega_2$ (we assume $\omega_1 > \omega_2$) and corresponding current amplitude $I_\sigma^p$ and $I_\delta^p$. Using the Hamilton equations $\dot{Q}_X = -\partial H_{JPC}/\partial\Phi_X$ and $\dot{Q}_Y = -\partial H_{JPC}/\partial\Phi_Y$, we can derive the equations of motion for the two modes $X$ and $Y$

$$\ddot{\Phi}_X + \kappa_a\dot{\Phi}_X + \omega_a^2\Phi_X + 2\Phi_Y[\frac{\chi_\sigma}{C_a}\cos(\Omega_\sigma t + \varphi_\sigma) + \frac{\chi_\delta}{C_a}\cos(\Omega_\delta t + \varphi_\delta)] \;=\; 2\epsilon_1\cos(\omega_1 t + \phi_1) \tag{8}$$

$$\ddot{\Phi}_Y + \kappa_b\dot{\Phi}_Y + \omega_b^2\Phi_Y + 2\Phi_X[\frac{\chi_\sigma}{C_b}\cos(\Omega_\sigma t + \varphi_\sigma) + \frac{\chi_\delta}{C_b}\cos(\Omega_\delta t + \varphi_\delta)] \;=\; 2\epsilon_2\cos(\omega_2 t + \phi_2) \tag{9}$$

where $\chi_\sigma = I_\sigma^p/(4\varphi_0)$ and $\chi_\delta = I_\delta^p/(4\varphi_0)$. The coefficients $\kappa_{a(b)} = \left(R_{a(b)}C_{a(b)}\right)^{-1}$ are the usual damping factors in RLC circuits, $\omega_{a(b)} = \sqrt{\frac{L_{a(b)}+L_J}{L_J L_{a(b)} C_{a(b}}}$ are the resonance frequencies of resonators renormalized by the quadratic terms in (4) and $\epsilon_{1(2)} = U_{1(2)}\kappa_{a(b)}$. Note that the presence of higher order spurious terms would make the resonance frequencies dependent on pump power and induce instabilities. Our circuit has a direct mechanical analog consisting of two coupled harmonic oscillators whose mutual coupling is parametrically driven. Following the usual treatment of a parametric amplifier, we impose the resonant tuning $\omega_1 = \omega_a$ and $\omega_2 = \omega_b$ and look for solutions of the form $\Phi_X = xe^{i\omega_1 t} + c.c.$ and $\Phi_Y = ye^{i\omega_2 t} + c.c.$. Keeping only the terms oscillating at $\omega_1$ and $\omega_2$, we obtain the phasors

$$x = \frac{-i\kappa_b\omega_2\tilde{\epsilon}_1 - \frac{\tilde{\chi}_\sigma}{C_a}\tilde{\epsilon}_2^* + \frac{\tilde{\chi}_\delta}{C_a}\tilde{\epsilon}_2}{\kappa_a\kappa_b\omega_1\omega_2 - \frac{\chi_\sigma^2}{C_aC_b} + \frac{\chi_\delta^2}{C_aC_b}} \tag{10}$$

$$y = \frac{-i\kappa_a\omega_1\tilde{\epsilon}_2 - \frac{\tilde{\chi}_\sigma}{C_b}\tilde{\epsilon}_1^* + \frac{\tilde{\chi}_\delta^*}{C_b}\tilde{\epsilon}_1}{\kappa_a\kappa_b\omega_1\omega_b - \frac{\chi_\sigma^2}{C_aC_b} + \frac{\chi_\delta^2}{C_aC_b}} \tag{11}$$

where $\tilde{\chi}_\delta = \chi_\delta e^{i\varphi_\delta}$, $\tilde{\chi}_\sigma = \chi_\sigma e^{i\varphi_\sigma}$ and $\tilde{\epsilon}_1 = \epsilon_1 e^{i\phi_1}$, $\tilde{\epsilon}_2 = \epsilon_2 e^{i\phi_2}$.

From the point of view of microwave circuits, rather than the local fluxes $\Phi_X$ and $\Phi_Y$ and voltages $U_1$ and $U_2$, it is more convenient to introduce the normalized amplitudes of the incoming and outgoing modes $a_{1(2)}^{\text{in}}$ and $a_{1(2)}^{\text{out}}$ at ports 1 and 2. This transformation is described in details in the Methods section. As a result, we can express the equations (10) and (11) in a very concise way by introducing the scattering matrix $S_{\text{JPC}}$ of the JPC.

$$\begin{pmatrix} a_1^{\text{out}}[\omega_1] \\ a_1^{*\text{out}}[-\omega_1] \\ a_2^{\text{out}}[\omega_2] \\ a_2^{*\text{out}}[-\omega_2] \end{pmatrix} = \begin{pmatrix} r_1 & 0 & t_1 & s_1 \\ 0 & r_1 & s_1^* & t_1^* \\ t_2 & s_2 & r_2 & 0 \\ s_2^* & t_2^* & 0 & r_2 \end{pmatrix} \cdot \begin{pmatrix} a_1^{\text{in}}[\omega_1] \\ a_1^{*\text{in}}[-\omega_1] \\ a_2^{\text{in}}[\omega_2] \\ a_2^{*\text{in}}[-\omega_2] \end{pmatrix} \tag{12}$$

where the coefficients are given, at the resonant tuning, by $r_1 = r_2 = r = \frac{1-|\rho_\delta|^2+|\rho_\sigma|^2}{1+|\rho_\delta|^2-|\rho_\sigma|^2}$, $t_1 = t_2^* = t = \frac{2i\rho_\delta}{1+|\rho_\delta|^2-|\rho_\sigma|^2}$ and $s_2 = s_1 = s = \frac{-2i\rho_\sigma}{1-|\rho_\delta|^2+|\rho_\sigma|^2}$ and where we have introduced the reduced pump currents $\rho_\delta = \frac{\tilde{\chi}_\delta}{\sqrt{C_aC_b\kappa_a\kappa_b\omega_1\omega_2}}$ and $\rho_\sigma = \frac{\tilde{\chi}_\sigma}{\sqrt{C_aC_b\kappa_a\kappa_b\omega_1\omega_2}}$. The three coefficients $r$, $t$ and $s$ satisfy the relation $|r|^2 + |t|^2 - |s|^2 = 1$. The form of this scattering matrix is in fact quite remarkable. As we show in the Methods section, $S_{\text{JPC}}$ has the exact minimal form required to perform phase preserving amplification with minimum added noise and noiseless frequency conversion. This is the consequence of (i) the dispersive nature of the operation of the device and (ii) the number of modes having been kept minimal. The same matrix form is obtained with the series circuit of Fig. 2b, albeit with different expressions for the $\rho's$.

The case $\rho_\delta = 0$ corresponds to the optimal amplification operation described in Fig 2c. The coefficients $|r|$ and $|s|$ can then be written as $|r| = \sqrt{G} = \frac{1+|\rho_\sigma|^2}{1-|\rho_\sigma|^2}$ and $|s| = \sqrt{G-1} = \frac{2\rho_\sigma}{1-|\rho_\sigma|^2}$. Amplification ($G \gg 1$) is obtained when the reduced pump current $\rho_\sigma$ approaches 1 from below. The diagonal term $r$ can be seen as a photon "cis-gain" characteristic of 1-port reflection amplifier operation. From the point of view of each port separately, the device behaves as a sort of ideal negative resistance: the incoming wave at either port is reflected with a power gain $G$ and its phase is preserved, when the signal at the other port is zero. A circulator is needed to separate the outgoing wave from the incoming one. The non-diagonal term $s$ can be seen as a photon "trans-gain" between different ports. Since it couples conjugated mode amplitudes $a^{\text{out}}_{1(2)}$ and $a^{*\text{in}}_{2(1)}$, the device behaves as a phase conjugating frequency converter with power gain $G-1$ [6]. In particular, this operation can be used to mix down a signal from high frequency $\omega_1$ to low frequency $\omega_2$. The remarkable feature here is the presence of photon gain. SIS mixers operating from the quasiparticle branch of a tunnel junction are so far the only known practical examples of mixers with gain, and they can operate quite close to the quantum limit [27].

The case $\rho_\sigma = 0$ corresponds to a conversion mode where an incoming mode at one port is partially reflected and partially converted into the second mode (Fig 2d). This operation is analogous to the one performed by a beam splitter but with the peculiarity that the frequency of the transmitted signal is converted when modes 1 and 2 have different frequencies $\omega_1$ and $\omega_2$. The device conserves the total number of incoming photons ($|r|^2 + |t|^2 = 1$), whereas the energy is conserved only if $\omega_1 = \omega_2$. Pure frequency conversion with unity gain can be obtained when $|\rho_\delta| = 1$. Although both modes of operation make frequency conversion possible, there are some fundamental differences between the two processes. The pure converter case allows to convert frequency with no added noise and without any reflection. On the other hand, the phase conjugating conversion of the amplification mode has the advantage of enabling photon gain.

**Noise of the JPC**

Let us now analyze the noise properties of the JPC for the two different cases of operation. Assuming thermal equilibrium with $T \ll \frac{\hbar\omega}{k_B}$, each port is fed at its input with half a photon of noise arising from vacuum fluctuations. Therefore, the total output noise power emitted by each port in units of photon number per mode is

$$N^{\text{out}} = \frac{1}{2}|r|^2 + \frac{1}{2}|t|^2 + \frac{1}{2}|s|^2 = \frac{1}{2}(2(|r|^2 + |t|^2) - 1)$$

In the case of amplification ($t = 0$) with large gain ($|r| \gg 1$), the noise referred back to the input is

$$N^{\text{in}}_{\text{eff}} = N^{\text{out}}/|r|^2 (\simeq N^{\text{out}}/|s|^2) = 1 + \frac{-1}{2|r|^2} \rightarrow 1$$

Although each port is fed at its input with only half photon of noise, after amplification the total output noise at each port is equivalent to one photon at the input ($N^{\text{in}}_{\text{eff}} \rightarrow 1$). This is an illustration of Caves' theorem [3]: the noise added by the amplification process to the vacuum noise already present at the input port is equivalent to half a photon ($N^{\text{in}}_{\text{add}} \rightarrow \frac{1}{2}$).

In the pure converter case ($|s| = |r| = 0$, $|t| = 1$), the noise referred back to input is

$$N^{\text{in}}_{\text{eff}} = N^{\text{out}}/|t|^2 = \frac{2|t|^2 - 1}{2|t|^2} = \frac{1}{2}$$

In this case, the output noise is identical to the input noise (half photon) and no noise is added during the process ($N^{\text{in}}_{\text{add}} = 0$). The photon number gain is unity, despite the fact that it is possible to have power gain when the frequency is up-converted.

**The general case of arbitrary detuning**

Detuning the signal frequencies from the resonance frequencies of the resonators ($\omega_1 \neq \omega_a$ and $\omega_2 \neq \omega_b$) complicates the expression of $S_{JPC}$ but retains the phase-preserving quantum limited operation to be reached when $\rho_\delta = 0$ or $\rho_\sigma = 0$. In the general case ($r \neq 0$, $s \neq 0$ and $t \neq 0$) the matrix does not retain the phase preserving property.

In the amplification mode of operation ($\rho_{\delta=0}$), the coefficients of $S_{\mathrm{JPC}}$ are given by

$$r_{1,2} = -\frac{(\vartheta_{2,1}+i)(\vartheta_{1,2}+i) - |\rho_\sigma|^2}{(\vartheta_{2,1}+i)(\vartheta_{1,2}-i) - |\rho_\sigma|^2} \quad \text{and} \quad s_{1,2} = \frac{-2i\rho_\sigma}{(\vartheta_{2,1}+i)(\vartheta_{1,2}-i) - |\rho_\sigma|^2} \tag{13}$$

where $\vartheta_1 = \frac{(\omega_1^2-\omega_a^2)Q_a}{\omega_a^2}$ and $\vartheta_2 = \frac{(\omega_2^2-\omega_b^2)Q_b}{\omega_b^2}$. Here we have introduced the quality factor of the resonators $Q_a = \frac{\omega_a}{\kappa_a}$ and $Q_b = \frac{\omega_b}{\kappa_b}$. Figure 3a shows a typical example of gain curves for different values of $|\rho_\sigma|$. In the large gain limit the expression of $r_{1,2}$ reduces to a Lorentzian form

$$r_{1,2} \simeq \frac{\sqrt{G}}{\sqrt{1 + G(\frac{Q_a}{\omega_a} + \frac{Q_b}{\omega_b})^2(\omega_{1,2} - \omega_{a,b})^2}} \tag{14}$$

The -3dB bandwidth of the amplifier is thus

$$B = \frac{2}{\sqrt{G}}\Big(\frac{Q_a}{\omega_a} + \frac{Q_b}{\omega_b}\Big)^{-1} \tag{15}$$

We arrive here at an important result: the bandwidth of the amplifier is inversely proportional to the amplitude gain $\sqrt{G}$. This feature is a general property of parametric amplifiers. At this point, we would like to stress that the pump frequency $\Omega_\sigma$ is an additional tuning parameter, which allows to displace the center of the signal bandwidth within the larger tuning bandwidth of the resonators. The case of an arbitrary detuning for the conversion mode of operation is treated in the Methods section.

**Practical issues: gain, bandwidth, dynamic range and stability.**

We now analyze some practical issues and show that we can build a practical device which would be useful for many different applications. The questions of power gain and bandwidth are central

and are intimately related. Ideally, the amplified noise should be much larger than the noise of the following amplifier in the measurement chain. For a quantum limited amplifier working at GHz frequencies and assuming the best "state of the art" commercial device as a following amplifier (a noise temperature of a few K is typical), the power gain has to be at least 20 dB, although of course a smaller power gain can still lead to an improvement in the overall system noise temperature. To optimise the ability of the amplifier to follow fast signals, a bandwidth around the carrier frequency as large as possible is sough. However, as shown by relation (15), the parametric coupling imposes the signal bandwidth to decrease with the amplitude gain. Although the gain of the JPC should in principle reach any arbitrarily large value when $|\rho_\sigma|$ approaches 1 sufficiently close, two limitations can occur. The first limitation is that when $|\rho_\sigma| \to 1^-$, the fraction of the pump current feeding the junctions should remain well below the Z mode critical current $I_0' = I_0 \cos\frac{\Phi}{4\varphi_0} = \frac{I_0}{\sqrt{2}}$, in order for the parametric amplification to remain stable (higher order non-linear terms invade the behavior of the device as the critical current is reached). It is useful to rewrite the expression of $|\rho_\sigma|$ as

$$|\rho_\sigma| = \frac{1}{4}\sqrt{Q_a Q_b p_a p_b}\frac{I_\sigma^p}{I_0'}$$

in which we introduce the participation ratios of the inductance of the Josephson ring modulator to the resonators inductance $p_{a,b} = \frac{L_{a,b}}{L_J + L_{a,b}}$ in the parallel case and $p_{a,b} = \frac{L_J}{L_J + L_{a,b}}$ in the series case. Since each junction receives a fourth of the total pump current, the first limitation thus translates into

$$\sqrt{Q_a Q_b p_a p_b} > 1 \tag{16}$$

Figure 3b shows the constraints on the JPC bandwidth and gain $G$ imposed by this limitation. This figure illustrates the impossibility of obtaining at the same time a high gain value and a large bandwidth with a parametric amplifier. Although this figure would seem to suggest that the

participation ratio $p_a$ and $p_b$ should be as high as possible, in practice dynamic range considerations limit this possibility (see below). The second limitation arises from the fact that the sum of the resonator energies, each being weighted by its participation ratio, cannot exceed the Josephson energy. We write this new condition as

$$E_a p_a + E_b p_b < E_J \tag{17}$$

In particular, the amplified zero-point quantum noise cannot exceed the Josephson energy

$$G\hbar(p_a\omega_a + p_b\omega_b)/2 < E_J \tag{18}$$

Taking $p_a = p_b = p$ to simplify the algebra we can rewrite Eq. (18) as

$$G < \frac{Z_Q}{Z_c} p^{0,-2} \tag{19}$$

where $Z_Q = \frac{\varphi_0^2}{\hbar} = \frac{\hbar}{(2e)^2} \simeq 1\text{k}\Omega$ is the quantum of impedance and $Z_c = \frac{\omega_a+\omega_b}{\sqrt{C_a C_b}\omega_a\omega_b}$ is an impedance characterising the resonators. Using a conventional microwave technology, this impedance would be of the order of 50Ω.The exponents zero and -2 refer to the parallel and series case respectively.

The power gain × bandwidth product is an important characteristics which determines the total flow of information that can be processed by the amplifier. Equations (16) and (19) can be combined to obtain an important bound on this product

$$G \times B = \frac{2\omega}{Q} G^{1/2} < 2\omega \sqrt{\frac{Z_Q}{Z_c}} p^{+1,0} \tag{20}$$

where we have taken $\omega_a$=$\omega_b$=$\omega$ to simplify the algebra. Since $p < 1$, the final upper bound on the gain×bandwidth product is thus $G \times B < 2\omega\sqrt{\frac{Z_Q}{Z_c}}$. Thus, both parallel and perpendicular circuits have the same limitation on the power gain ×bandwidth product. However, in the case of the parallel

circuit the maximum gain is strongly constrained by relation (19). Therefore, the series case appears more favourable in most of the practical cases. Another important characteristic of an amplifier is its dynamic range, i. e., for a given gain, the maximum input power $P_{\max}$ that the device can amplify before it starts to saturate. The same considerations involving the maximum power produced by the device, as developed in relation (18), can be used to obtain the dynamic range:

$$2Gp\Big(\frac{P_{\max}}{B}+\frac{\hbar\omega}{2}\Big)<E_J \tag{21}$$

Therefore

$$P_{\max}<\frac{B}{2}\Big(\frac{E_J}{Gp}-\hbar\omega\Big) \tag{22}$$

However, when the input power becomes too large, our small amplitude approximation is no longer valid and higher non-linear terms in (6) start to play a role. Therefore, experimentally, the amplifier may saturate before reaching the theoretical value.

We now turn to the question of stability. The point $\rho_\sigma = 1$ corresponds to the onset of spontaneous self-oscillations of the system. Therefore, the JPC should be operated at a distance from this critical point safe in regards to fluctuations in pump drive power. But here, the situation is better controlled than in previous studies where optimization of gain would conflict with an increase of noise caused by the proximity of a poorly identified instability [28, 29, 30] whose influence might be difficult to avoid.

**Production of entangled signal pairs and dynamic cooling**

The gain of the JPC is high enough to potentially raise the level of quantum fluctuations at a much

higher than the level of the noise of the second amplifier in the chain. An interesting experiment consists in turning on the pump without feeding any signals at the input ports of the JPC. Quantum-mechanically, the pump can still produce output signals, which can be seen as arising from the amplification of zero-point motion fluctuations. Moreover, since the scattering matrix conserves the volume of the phase space, the amplified noise appearing at the two ports must be entirely correlated. The function which is performed is two mode squeezing[31]. As the output signals can have many real microwave photons, such a device could be used for analog quantum encryption[32].

Another interesting feature of the pure frequency converter mode of operation is that, unlike the amplifier mode, it has no added noise at the output. The JPC device operating in this case with a unity photon number "trans-gain" can swap the photons at the two ports and be used as a refrigerator. Suppose that the frequency at port 2 is much smaller than the frequency at port 1, which sees an environment cold in the sense $\hbar\omega_1 \gg k_B T_1$. Initially port 2 is seeing an environment which is hot in the sense $\hbar\omega_2 \ll k_B T_2$. When the JPC is operated, the photons at port 2 are shuttled to port 1 where they are evacuated, while zero-point photons from port 1 go in the other direction to replace the photons at port 2 imposing vanishing temperature. The cooling rate being $\dot{q} = k_B T_2 \kappa_b$, the refrigeration power is only of the order of 1pW at 4K and for a bandwidth of 1GHz, but it can be very useful for a high-Q resonator isolated from the thermal bath.

## Conclusion

The Josephson Parametric Converter would fill a niche which was up to now unavailable in the landscape of microwave processing devices, that of 3-wave mixing for non-degenerate parametric amplification operating at the quantum limit. Moreover, we would like to stress that the present level of control in the dynamics of tunnel junctions in resonant circuits, as demonstrated by recent

several successful operations [13, 14, 15, 33, 34], ensures that its realization is entirely within reach. This development would bring the subject of analog rf quantum signal processing (should we nickname it quantum radioelectricity ?) to a qualitatively new level.

Correspondence and requests for material should be address to M. D and N.B

This work was supported by NSA through ARO Grant No. W911NF-05-01-0365, the Keck foundation, and the NSF through Grant No. DMR-032-5580. M. H. D. acknowledges partial support from College de France.

## Methods

### Transformation of local fluxes and voltages to traveling waves

In the circuit of figure 2a, the local fluxes and voltages can be expressed as a function of the amplitude of the incoming and outgoing modes $A^{in}$ and $A^{out}$ at ports 1 and 2 using the following relations

$$A_1^{\rm in} + A_1^{\rm out} = \frac{V_1 - V_2}{\sqrt{R_a}} = \frac{i\omega_1 x}{\sqrt{R_a}}; \quad A_1^{\rm in} + A_1^{\rm out} = \frac{V_4 - V_3}{\sqrt{R_b}} = \frac{i\omega_2 y}{\sqrt{R_b}}; \quad A_1^{\rm in} = \frac{U_1}{2\sqrt{R_a}} : \quad A_2^{\rm in} = \frac{U_2}{2\sqrt{R_b}}$$

$A^{\rm in}$ and $A^{\rm out}$ are expressed in square root of watts. We can now define the normalized amplitude $a^{\rm in}$ and $a^{\rm out}$ expressed in square root of photon number per unit time.

$$a_1^{\rm in} = \frac{A_1^{\rm in}}{\sqrt{\hbar\omega_1}}; \quad a_2^{\rm in} = \frac{A_2^{\rm in}}{\sqrt{\hbar\omega_2}}; a_1^{\rm out} = \frac{A_1^{\rm out}}{\sqrt{\hbar\omega_1}}; \quad a_2^{\rm out} = \frac{A_2^{\rm out}}{\sqrt{\hbar\omega_2}}$$

At this point, the normalized ampitudes are still classical variables. The passage to the creation and annihilation operators is performed by the simple replacement $a \rightarrow \hat{a}$ and $a^* \rightarrow \hat{a}^\dagger$.

### Minimal scattering matrix for quantum information processing

In order to perform information processing at the quantum limit, a device must fulfill requirements that impose constraint of its scattering matrix $S$. In this section we derive the minimal form of $S$ to perform phase preserving amplification with minimal added noise and noiseless frequency conversion

in the case of a device involving only two modes. Following a route similar but not identical to that pioneered by Caves, we introduced the generalized scattering matrix $S$ of a linear microwave device which relates input and output modes at its different ports.

$$\Lambda^{out} = S \cdot \Lambda^{in}$$

Here we have introduced the mode amplitude input and output vectors

$$\Lambda^{in} = \begin{pmatrix} a_1^{\text{in}} \\ a_1^{*\text{in}} \\ \vdots \\ a_n^{\text{in}} \\ a_n^{*\text{in}} \\ \end{pmatrix} \quad ; \quad \Lambda^{out} = \begin{pmatrix} a_1^{\text{out}} \\ a_1^{*\text{in}} \\ \vdots \\ a_n^{\text{in}} \\ a_n^{*\text{in}} \\ \end{pmatrix}$$

where the symbol $^*$ denotes the complex conjugation. The $a_n$ are normalized mode amplitudes expressed in square root of photon number per unit time. Although they are at first treated as classical scalar fields, they can, in a later quantum mechanical treatment, be formally replaced by annihilation ($a_n \rightarrow \hat{a}_n$) and creation ($a_n^* \rightarrow \hat{a}_n^\dagger$) operators. Both $a$ and $a^*$ have to be present in the input and output vectors because of possible phase conjugating processes coupling an $a^{out}$ to an $a^{*in}$. In the case of a device with two ports, the most general matrix has only 8 independent complex coefficients.

$$S = \begin{pmatrix} r_1 & u_1 & t_1 & s_1 \\ u_1^* & r_1^* & s_1^* & t_1^* \\ t_2 & s_2 & r_2 & u_2 \\ s_2^* & t_2^* & u_2^* & r_2^* \end{pmatrix}$$

Our requirement of information processing at the quantum limit implies that the scattering matrix must describe a canonical transformation that preserves the commutation relations of the bosonic fields $[\hat{a}_n^{\text{out}}, \hat{a}_n^{\dagger\text{out}}] = [\hat{a}_n^{\text{in}}, \hat{a}_n^{\dagger\text{in}}]$. Mathematically, this is translated by the property of symplecticity of the $S$ matrix [35, 36]

$${}^T SJS = J$$

where

$$J = \begin{pmatrix} 0 & 1 & 0 & 0 \\ -1 & 0 & 0 & 0 \\ 0 & 0 & 0 & 1 \\ 0 & 0 & -1 & 0 \end{pmatrix}$$

In order to perform phase preserving amplification, we need to impose that the reflection at each port separately preserves the phase of the signal (i.e. a phase shift of the incoming wave results in an identical phase shift of the outgoing wave). That implies that $u_1 = u_1^* = u_2 = u_2^* = 0$. Finally, without loss of generality we can impose the modulus of the reflection coefficients to be identical at each port ($|r_1| = |r_2| = |r|$). It follows that $S$ has the minimal form

$$S = \begin{pmatrix} |r|e^{i\alpha_1} & 0 & |t|e^{i\beta_1} & |s|e^{i\gamma_1} \\ 0 & |r|e^{-i\alpha_1} & |s|e^{-i\gamma_1} & |t|e^{-i\beta_1} \\ -|t|e^{i(\alpha_1+\alpha_2-\gamma_1)} & |s|e^{i(\alpha_2-\alpha_1+\beta_1)} & |r|e^{i\alpha_2} & 0 \\ |s|e^{-i(\alpha_2-\alpha_1+\beta_1)} & -|t|e^{-i(\alpha_1+\alpha_2-\gamma_1)} & 0 & |r|e^{-i\alpha_2} \end{pmatrix}$$

where the coefficients are linked by the relation $|r|^2 + |t|^2 - |s|^2 = 1$.

The case $s = 0$ corresponds to a conversion operation where an incoming mode at one port is partially reflected and partially converted into the second mode. Since $|r|^2 + |t|^2 = 1$, the total number of photons is conserved during the process. The case $t = 0$ corresponds to an amplification operation since the total number of photons is not longer conserved ($|r|^2 + |s|^2 \neq 1$). Therefore, $|r|$ can take any value larger than one, the phase of the signal being preserved. This matrix has the simplest form for performing phase preserving amplification and frequency conversion at the quantum limit.

**Case of arbitrary detuning for the conversion mode of operation**

In the conversion mode of operation ($\rho_{\sigma=0}$)

$$r_{1,2} = \frac{(\vartheta_{2,1} - i)(\vartheta_{1,2} + i) - |\rho_\delta|^2}{(\vartheta_{2,1} - i)(\vartheta_{1,2} - i) - |\rho_\delta|^2} \quad \text{and} \quad t_{1,2} = \frac{-2i\rho_\delta}{(\vartheta_{2,1} - i)(\vartheta_{1,2} - i) - |\rho_\delta|^2} \tag{23}$$

where $\vartheta_1 = \frac{(\omega_1^2-\omega_a^2)Q_a}{\omega_a^2}$ and $\vartheta_2 = \frac{(\omega_2^2-\omega_b^2)Q_b}{\omega_b^2}$.

---


[1] Shimoda, K., Takahasi, H. and C. H. Townes, C. H. Fluctuations in Amplification of Quanta with Application to Maser Amplifiers. J. Phys. Soc. Jpn. **12**, 686-700 (1957).

[2] Haus, H. A. and Mullen, J. A. Quantum Noise in Linear Amplifiers. Phys. Rev. **128**, 2407-2413 (1962).

[3] Caves, C. M. Quantum limits on noise in linear amplifiers. Phys. Rev. D **26**, 1817-1839 (1982).

[4] Tien, P. K. Parametric Amplification and Frequency Mixing in Propagating Circuits. J. Appl. Phys. **29**, 1347-1357 (1958).

[5] Louisell, W. H. Coupled mode and parametric electronics. John Wiley, New York (1960).

[6] Louisell, W. H., Yariv, A. and Siegman, A. E. Quantum Fluctuations and Noise in Parametric Processes. I. Phys. Rev. **124**, 1646-1654 (1961).

[7] Gordon, J. P., Louisell, W. H. and Walker, L. R. Quantum Fluctuations and Noise in Parametric Processes. II. Phys. Rev. **129**, 481-485 (1963).

[8] André, M-O., Mück, M., Clarke, J., Gail, J., Heiden, C. Radio-frequency amplifier with tenth-kelvin noise temperature based on a microstrip direct current. Appl. Phys. Lett. **75**, 698-700 (1999).

[9] Spietz, L., Irwin, K., Aumentado, J. Input impedance and gain of a gigahertz amplifier using a dc superconducting quantum interference device in a quarter wave resonator. Appl. Phys. Lett., **93**, 082506 (2008).

[10] Yurke, B. et al. Observation of parametric amplification and deamplification in a Josephson parametric amplifier. Phys. Rev. A **39**, 2519-2533 (1989).

[11] Yurke, B. Observation of 4.2-K equilibrium-noise squeezing via a Josephson-parametric amplifier. Phys. Rev. Lett. **60**, 764-767 (1988).

[12] Movshovich, R. et al. Observation of zero-point noise squeezing via a Josephson-parametric amplifier. Phys. Rev. Lett. **65**, 1419-1422 (1990).

[13] Wallraff, A. et al. Strong coupling of a single photon to a superconducting qubit using circuit quantum electrodynamics. Nature **431**, 162-167 (2004).

[14] Lupaşcu, A., Saito, S., Picot, T., de Groot, P. C., Harmans, C. J. P. M., Mooij, J. E. Quantum

non-demolition measurement of a superconducting two-level system. Nature Physics **3**, 119-125 (2007).

[15] Mika A. Sillanpää, M. A., Park, J. I., Simmonds, R. W. Coherent quantum state storage and transfer between two phase qubits via a resonant cavity. Nature **449**, 438-442 (2007).

[16] Majer, J. et al. Coupling superconducting qubits via a cavity bus. Nature, **449**, 443-447 (2007).

[17] Castellanos-Beltran, M. A. and Lehnert, K. W. Widely tunable parametric amplifier based on a superconducting quantum interference device array resonator. Appl. Phys. Lett. **91**, 083509 (2007).

[18] Castellanos-Beltrana, M. A. Irwin, K. D., Hilton, G. C., Vale, L. R., Lehnert, K. W. Amplification and squeezing of quantum noise with a tunable Josephson metamaterial. Nature Phys. , **4**, 928-931 (2008).

[19] Tholeń, E. A. Nonlinearities and parametric amplification in superconducting coplanar waveguide resonators. Appl. Phys. Lett. **90**, 253509, (2007).

[20] Yamamoto, T., Inomata, K., Watanabe, M., Matsuba, K., Miyazaki, T., Oliver, W. D., Nakamura, Y. and Tsai, J. S. Flux-driven Josephson parametric amplifier. Appl. Phys. Lett **93**, 042510 (2008).

[21] Zhang Q., Ruskov R., Korotkov. A. N., Continuous quantum feedback of coherent oscillations in a solid-state qubit. Phys. Rev. B **72**, 245322 (2005).

[22] Korotkov. A. N., Simple quantum feedback of a solid-state qubit. Phys. Rev. B **71**, 201305 (2005).

[23] D.M. Pozar, "Microwave Engineering", (Wiley, 2005), p. 629.

[24] Devoret, M. H. Quantum fluctuations in electrical circuits, Quantum Fluctuations : Les Houches Session LXIII, Elsevier, Amsterdam (1997).

[25] Yurke, B. and Denker, J. S. Quantum network theory. Phys. Rev. A **29**, 1419-1437 (1984).

[26] Caldeira, A. O. and Legget, A. J. Quantum Tunneling in a Dissipative System. Ann. Phys. **149**, 374-456 (1983).

[27] Mears, C. A Quantum-limited heterodyne detection of millimeter waves using superconducting tantalum tunnel junctions. Appl. Phys. Lett. **57**, 2487-2489 (1990).

[28] Wahlstein, S., Rudner, S., and Claeson, T. Arrays of Josephson tunnel junctions as parametric amplifiers. J. Appl. Phys. **49**, 4248-4263 (1979).

[29] Mygind, N. , Perdersen, F., Soerensen, O. H., Dueholm, B., Levinsen, M. T. Low-noise parametric amplification at 35 GHz in a single Josephson tunnel junction. Appl. Phys. Lett. **35**, 91-93 (1979).

[30] Bryant, P., Wiesenfeld, K. and McNamara, B. Noise rise in parametric amplifiers. Phys. Rev. B **36**, 752-755 (1987).

[31] Bjork, G. and Yamamoto, Y. Generation of nonclassical photon states using correlated photon pairs and linear feedforward. Phys. Rev. A **37**, 4229-4239 (1984).

[32] Grosshans, F. and Grangier, P. Continuous Variable Quantum Cryptography Using Coherent States. Phys. Rev. Lett. **88**, 057902 (2002).

[33] Siddiqi I. et al. RF-Driven Josephson Bifurcation Amplifier for Quantum Measurement. Phys. Rev. Lett. **93**, 207002 (2004).

[34] Metcalfe, M. et al. Measuring the decoherence of a quantronium qubit with the cavity bifurcation amplifier. Phys. Rev. B **76**, 174516 (2007).

[35] Arvind, Dutta Jawaharlal, B., Mukunda N. and Simon, R. The Real Symplectic Groups in Quantum Mechanics and Optics Xiv:quant-ph/9509002v3 (1995).

[36] Guillemin, V. and Sternberg, S. Symplectic Techniques in Physics. Cambridge University Press, (1984).

**Fig 1.** Electrical modes and energy states of the Josephson ring modulator. a) The Josephson ring modulator consists of four nominally identical Josephson junctions ($a$, $b$, $c$ and $d$) and has four orthogonal electrical modes. The two differential modes $X$,$Y$ and the common mode $Z$ are coupled to the junctions whereas the 4th mode $W$ remains uncoupled. b) Energy states of the ring modulator. There are 4 stable states satisfying the relation $\delta_a + \delta_b + \delta_c + \delta_d = n\frac{2\pi\Phi}{\Phi_0}$ where $\delta_i$ is the gauge invariant phase of the junction $i$. Each state is $4\Phi_0$ periodic as a function of the flux $\Phi$ through the loop but the envelope (blue line) of the lowest energy remains $\Phi_0$ periodic. Other energy extremum states are not represented here. At point $a$, the device can produce a pure non-linear coupling term $\Phi_X\Phi_Y\Phi_Z$ whose contamination is only of the type $\Phi_X^2 + \Phi_Y^2 + \Phi_Z^2$. Point $a$ actually corresponds to two degenerate states separated by an energy barrier whose height is $2(\sqrt{2}-1)E_J$. At point $b$, there is no contamination and the non-linearity is of the purest form, but it would be very difficult to stabilise the device in an excited state.

**Fig 2.** Description of the Josephson Parametric Converter. a) Lumped element schematic of the parallel JPC. The device is based on a ring modulator coupled to two parallel $LC$ resonators corresponding to the two differential modes $X$ and $Y$. The common mode $Z$ is driven by a current source $I^p$. Both resonators are coupled to external drives. b) Lumped element schematic of the series JPC. c) Scattering representation of the JPC in the case of amplification operation. Here the white arrows denote the conjugation operation since the non diagonal terms of the scattering matrix couples $a^{\text{out}}$ to $a^{*\text{in}}$. d) Scattering representation of the JPC in the case of the pure conversion operation.

**Fig 3.** Gain of the JPC. The figure displays in color scale the gain $r_1$ in the amplification mode as a function of the normalised input frequency $\omega_1/\omega_a$ for different values of $|\rho_\sigma|$ (from 0.6 to 0.99). In this example, $Q_a = 50$ and the damping factors are taken to be identical for the two resonators($\omega_a/Q_a$=$\omega_b/Q_b$).

**Fig 4.** Main constraint on the gain×bandwidth product of the JPC. The figure displays in color scale the pump current in the junction, normalised by the $Z$ mode critical current, as a function of the relative bandwith $B/\omega_a$ and the gain G. The brown area corresponding is not accessible for the JPC since in this region, the pump current in the junction always exceeds their critical current. The different contours correspond to the various limitations obtained for different participation ratios $p_a$ and $p_b$.

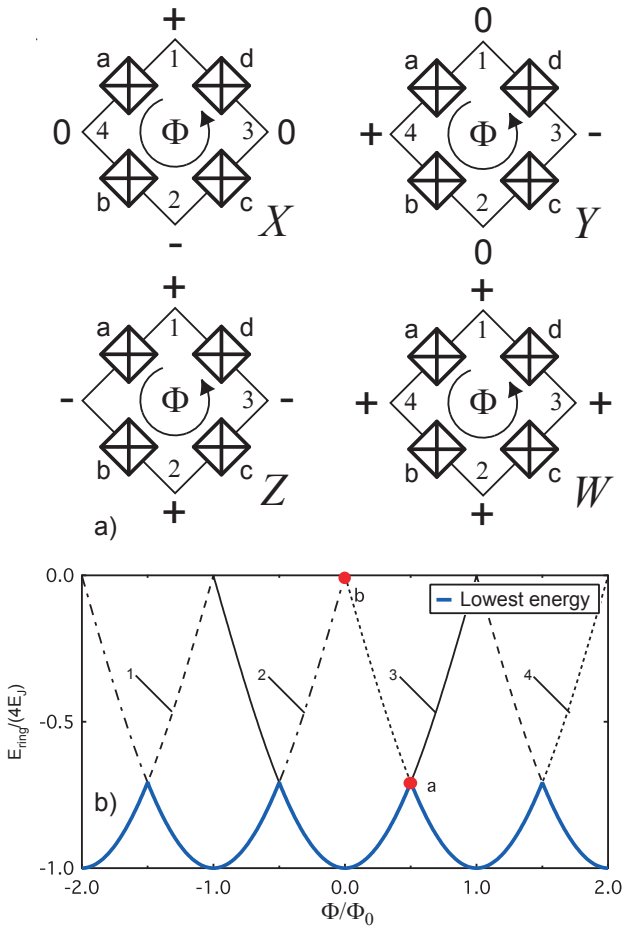
a
d
b
c
1
2
3
4
Φ
X
Y
Z
W
a)
b)
Lowest energy
$E_{ring}/(4E_J)$
$\Phi/\Phi_0$
0.0
-0.5
-1.0
-2.0
-1.0
0.0
1.0
2.0

FIG. 1:

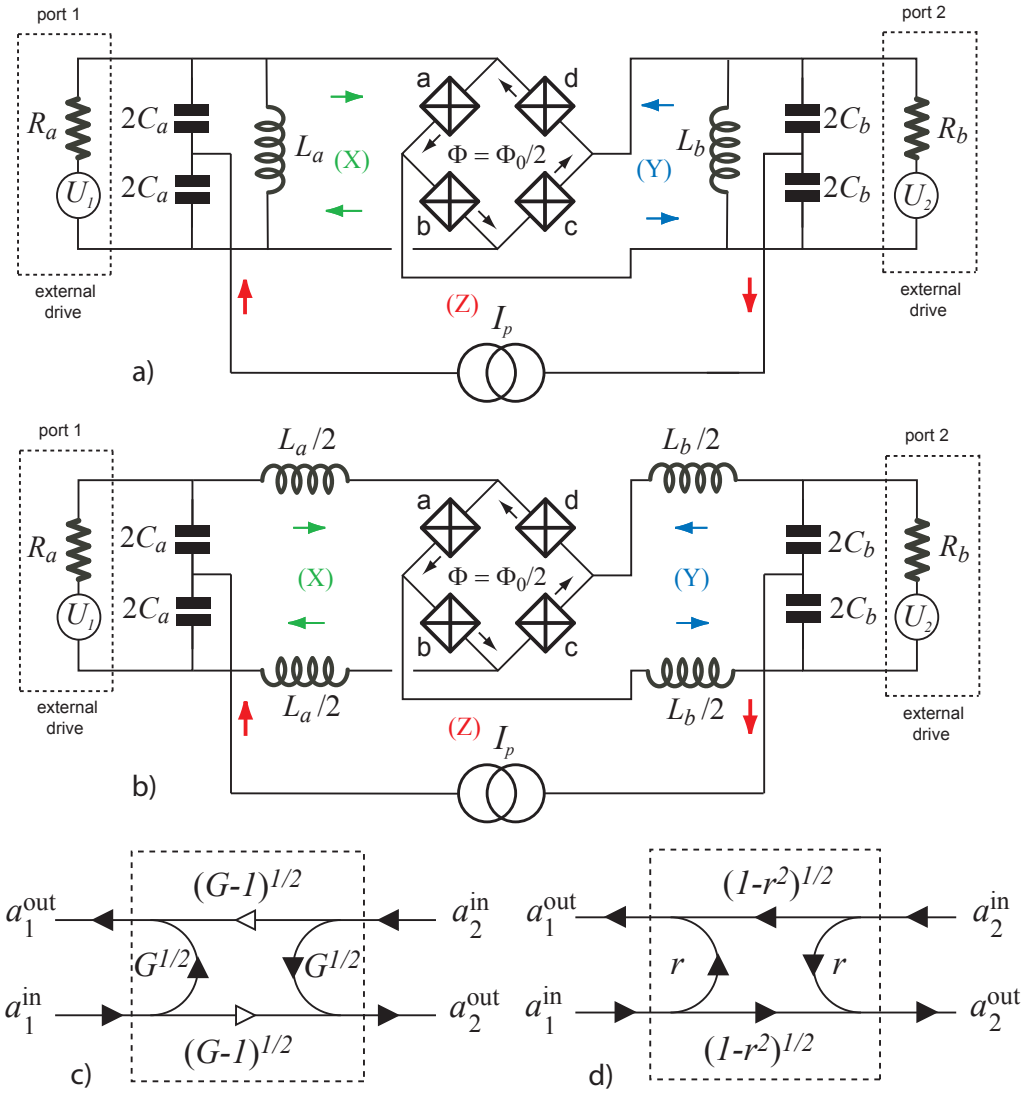
port 1
port 2
$R_a$
$2C_a$
$2C_a$
$U_1$
$L_a$ (X)
a
d
b
c
$\Phi = \Phi_0/2$
(Y)
$L_b$
$2C_b$
$2C_b$
$R_b$
$U_2$
external drive
external drive
(Z) $I_p$
a)
$L_a/2$
$L_b/2$
$L_a/2$
$L_b/2$
b)
$(G\text{-}1)^{1/2}$
$G^{1/2}$
$G^{1/2}$
$(G\text{-}1)^{1/2}$
$a_1^{out}$
$a_2^{in}$
$a_1^{in}$
$a_2^{out}$
c)
$(1\text{-}r^2)^{1/2}$
$r$
$r$
$(1\text{-}r^2)^{1/2}$
d)

FIG. 2:

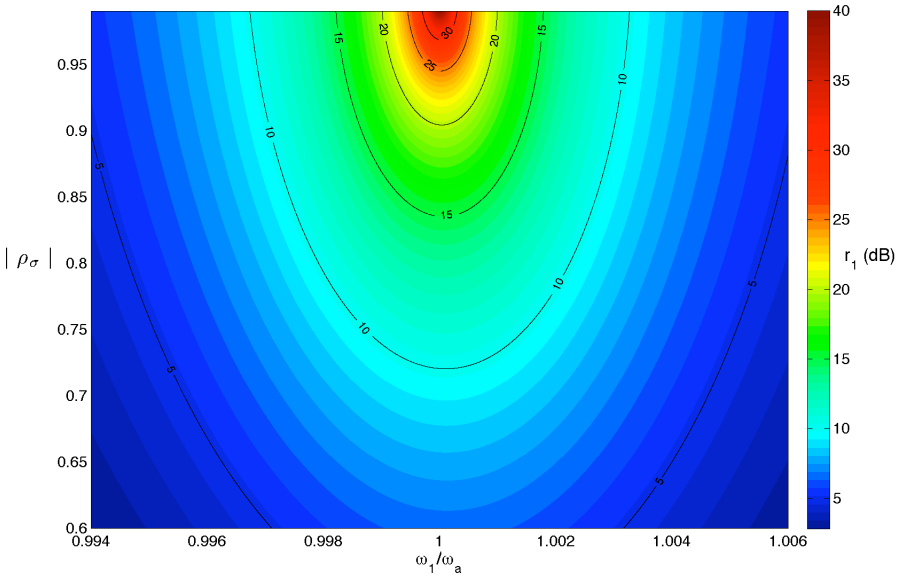
| ρσ |
ω1/ωa
r1 (dB)

FIG. 3:

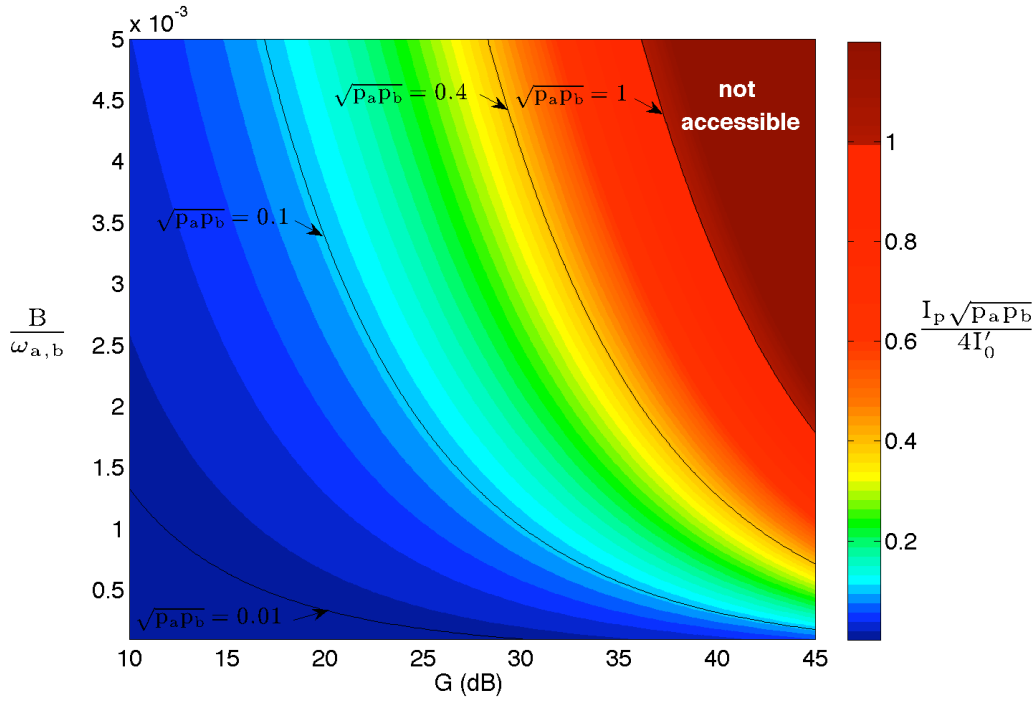
x 10-3
not accessible
√(pa pb) = 0.4
√(pa pb) = 1
√(pa pb) = 0.1
√(pa pb) = 0.01
B / ωa,b
G (dB)
Ip √(pa pb) / 4I'0

FIG. 4: